Compound Fault Diagnosis for Cooling Dehumidifier Based on RBF Neural Network Improved by Kernel Principle Component analysis and Adaptive Genetic Algorithm

Yunguang Gao (yung8791@126.com)
Hunan Trinity Industrial Vocational and Technical College https://orcid.org/0000-0001-6118-0322
Changlin Ma
Xi'an Inst. of Hi-Tech
An Sheng
Hunan Trinity Industrial Vocational and Technical College

Research Article

Keywords: Cooling dehumidifier, Compound fault, RBF neural network, Kernel principle component analysis, Adaptive genetic algorithm

Posted Date: May 18th, 2022

DOI: https://doi.org/10.21203/rs.3.rs-1611461/v1

Compound Fault Diagnosis for Cooling Dehumidifier Based on RBF Neural Network Improved by Kernel Principle Component Analysis and Adaptive Genetic Algorithm

Yunguang Gao[1], Changlin Ma[2], An Sheng[1]

Hunan Trinity Industrial Vocational and Technical College, Changsha County, Changsha, China

Xi'an Research Inst. of Hi-Tech, Hongqing Town, Xi'an, China

Abstract: Developing fault diagnosis for the cooling dehumidifier is very important for improving the equipment reliability and saving energy consumption. This paper mainly studies and explores the compound fault diagnosis for the cooling dehumidifier. Firstly, the dehumidifier data acquisition system is built, which can be applied to the data acquisition, work status simulation, and fault diagnosis. Secondly, a compound fault diagnosis model based on radial basis function neural network (RBFNN) improved by kernel principle component analysis (KPCA) and adaptive genetic algorithm (AGA) is proposed. Aiming at the problems that the selection of RBF width depends on expert knowledge, the network structure scale is large or the training speed is slow in the conventional RBFNN models, on the one hand, AGA and K-means clustering algorithm are employed to automatically optimize the RBF width, the number of hidden layer neurons and the neuron centers, which guarantees the model has small structure and fast computing speed on the premise of sufficient output precision; on the other hand, KPCA is used to reduce the dimension of the model input data, which not only effectively extracts the nonlinear features, but also further simplifies the network structure. Finally, the proposed method is validated and compared with the conventional models. The results show that this proposed model can not only be effectively applied to the dehumidifier compound fault diagnosis, but also has prominent application advantages.

Keywords: Cooling dehumidifier; Compound fault; RBF neural network; Kernel principle component analysis; Adaptive genetic algorithm

1. Introduction

As a kind of heating, ventilating, air-conditioning and refrigeration (HVAC&R) equipment, the cooling dehumidifier is widely applied to the fields such as building, electronic and precision

---

[1] *Yunguang Gao is an assistant professor, An Sheng is a lecturer.*

[2] *Changlin Ma is a researcher. *Corresponding author e-mail: yung8791@126.com*

instrument which need to control the environment temperature and humidity. As the same as other HVAC&R equipment, it's hard to avoid faults occurring in the cooling dehumidifier refrigeration system. When the faults occur in the equipment, there would be some risks such as: (1) The work status can't meet the technical standard so far as to lose effectiveness; (2) The work performance falls down and the energy consumption goes up; (3) The refrigerant leaks so that destroys environment; (4) The work safety is affected by the fault, e.g., refrigeration compressor suction pressure rise. So developing fault detection and diagnosis (FDD) for cooling dehumidifier is very important for improving equipment work reliability, saving energy consumption, protecting environment, lowering safety risk, reducing equipment maintenance cost and extending equipment life [1]. The involved research literatures demonstrate the HVAC&R system can save 20%-30% energy consumption in the operation after adopting FDD technology and optimization management [2]. Katipamula and Brambley [3, 4] reviewed the FDD methods for HVAC&R equipment, they consider these methods involve two classes, one is model based and the other is process history dada based. The artificial neural network (ANN) model belongs to a classical black model which is one of methods based on process history data.

The cooling dehumidifier fault mainly includes electric fault and mechanical fault, and the latter occurrence frequency is higher than the former. The mechanical fault mainly occurs in the refrigeration system. The cooling dehumidifier refrigeration system fault can be basically divided into two classes, one is the catastrophic fault, and the other is light fault. The surveys indicate that the light fault frequently occurs and isn't easily perceived although it is less serious than the catastrophic fault. The common light fault includes evaporator fouled, condenser fouled, refrigerant insufficient, expansion valve fault, air flow line fault, cooling water line fault and so on. Due to the powerful coupling in the inner components, the nonlinear characteristic of dehumidifier system is obvious, thus there is some difficulty to accurately diagnose the fault. When the refrigeration system faults occur, the fault symptoms and reasons are often complex, the attributes can be concluded as: 1) the symptoms represented by fault are complex; 2) the fault reasons are complex; 3) the relationship between the fault symptoms and reasons are complex, one reason can arouse multiple symptoms, and multiple reasons can represent the same symptom; 4) it's hard to find the strict logical and quantitative relationship from the system parameters, i.e., there is some fuzziness in the system; 5) there are many inner parameters to be measured. From this it can be seen that there is some difficulty to build precise mathematic or physical model for cooling dehumidifier fault analysis and diagnosis. At the same time, the process complexity of fault occurring and developing also brings difficulty to determine the fault threshold. For the complex fault compounded of two or more single faults, there is even more difficulty to diagnose due to the parameters coupling and the more complex corresponding relationships between fault symptoms and reasons. It is also hard to find an effective method for diagnosing the cooling dehumidifier compound fault.

As a black-box model, ANN is a kind of method for fitting training data and optimizing performance parameter by input and output data. Due to the merit of high parallel disposing, nonlinear mapping, self-adapting and fault toleration, ANN is suitable for system identification and pattern recognition. The fault diagnosis can be attributed to pattern recognition problem in final, therefore ANN is widely applied to the fault diagnosis fields such as aerospace engineering, chemical industry, pharmacy, petroleum, and so on. In the HVAC&R field, methods based on ANN for diagnosis were widely studied and applied, e.g., Peitsman and Bakker [5] employed ANN and autoregressive with exogenous input (ARX) model to fault diagnosis for a reciprocating chiller; Haves et al. [6] proposed a method based on radial basis function neural network (RBFNN) and gradient regressive estimation to detect coil fouled and valve leakage faults of air handing unite (AHU); House et al. [7] employed 7 kinds of classification methods for AHU fault diagnosis and these methods performance were analyzed by contrast; Lee et al. [8] proposed a method based on general regression neural network (GRNN) for AHU FDD, the simulation result demonstrated the GRNN has high precision and reliability for the application to the nonlinear system such as AHU; Dun et al. [9] proposed a method based on ANN for Variable Air Volume (VAV) sensor fault diagnosis; Dun et al. [10] developed a method based on ANN and subtractive clustering analysis for AHU fault FDD; Fan et al. [11] proposed a hybrid FDD strategy for local system of AHU based on ANN and wavelet analysis; furthermore, there are many studies [12-14] focused ANN methods on performance prognosis and analysis for air-conditioning and the validity is proved by simulation or application. Gao et al. [15] proposed a nonlinear ARX model for cooling dehumidifier fault detection, but the fault diagnosis need to be aided by expert knowledge and the fault types study only focused on single fault.

Reviewing these literatures, in the method research aspect, the black-box model are employed widely, e.g., the ARX model and feed-forward ANN. The ARX model is theoretically suitable for dealing with linear problems, but HVAC&R system has obvious nonlinear characteristics; ANN has strong nonlinear processing ability, so it is more suitable for fault diagnosis of HVAC&R. The most used feed-forward ANN mainly includes back-propagation neural network (BPNN) and RBFNN, the RBFNN has higher generalization ability and learning efficiency than t BPNN, and it has no local minimum problem existed in BPNN[16, 17]. Although RBFNN has been applied relatively successfully in fault diagnosis, the conventional RBFNN models mainly have two problems in the training. One is the balance between network structure and output precision, in the condition of the RBF width is determined, the output precision will improve with the number of neurons increase, but the structure will become complex; when the number of neurons is reduced, the structure will be simplified, and the output precision will be decreased. The structure size will affect the RBFNN online computing speed; the other is the selection of model parameter, RBF width has an important impact on the performance of RBFNN, the conventional artificial selection method needs to be adjusted repeatedly by experiment, so the operation is cumbersome, if it is not selected properly, it will lead to poor application effect of RBFNN. To solve these problems, this paper employs adaptive genetic algorithm (AGA) and K-means clustering algorithm to optimize the RBFNN structure and parameter at the same time, which guarantees that the model has smaller structure and faster computing speed on the premise of sufficient output precision.

In the fault research aspect, most studies focus on single fault. When the compound fault occurs on the same time, it is harder to diagnose than the single fault due to the complex equipment parameters coupling. In fact, the compound fault composes of single fault will occur for the real equipment, so research on compound fault diagnosis is necessary in despite of that this work would be difficult and full of challenges. Employing the powerful nonlinear processing ability of RBFNN, the compound fault diagnosis can be decomposed single fault diagnosis.

Compound fault diagnosis usually requires higher sample dimension, which will increase the structure and computational complexity of ANN. In view of this problem, this paper employs the kernel principal component analysis (KPCA) method to reduce the input sample dimension, so as to further reduce the structure of RBFNN, remove the correlation between input variables and better extract the data sample feature.

Based on the two problems of conventional RBFNN models and compound fault research in the HVAC&R fault diagnosis field, this paper proposed an improved RBFNN model based on KPCA and AGA for the cooling dehumidifier compound fault diagnosis.

2. RBFNN

Moody and Darken [18] developed a novelty RBFNN based on multidimensional space interpolation disposed by radial basis function (RBF). The RBFNN is proposed according to human cerebrum cortical adjustment and overlap receive field, which is also named local receive field neural network. It is a simplified and abstract cerebrum model. The RBFNN is superior than BPNN on the approximation, classification and learning speed, so it is widely applied to the fields such as system identification and pattern recognition, and then it gained close attentions by many researchers [19].

2.1 RBFNN structure

The RBFNN is a kind of special three-players ANN of feed forward neural networks. The input player unit only transmits input signal to the hidden player; the hidden player unit characteristic function employs nonlinear radial function in order to make local response to the input stimulus signal; the output player unit makes linear combination of the hidden player unit function outputs. The RBFNN structure is shown as Fig.1.

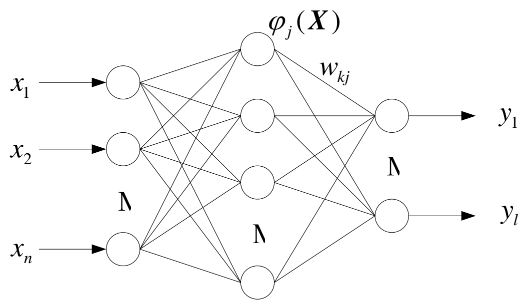

Fig.1 - RBFNN structure.

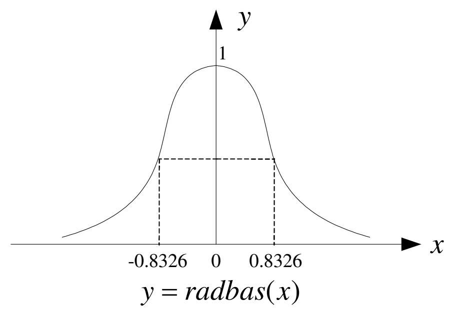

Fig.2 - Radial symmetry Guass function.

The radial symmetry Gauss function shown as Fig.2 is usually employed for the RBFNN nonlinear transmission function, and the transmission function in hidden player is shown as

$$\varphi_j(\boldsymbol{X}) = \exp[-(\| \boldsymbol{X} - \boldsymbol{C}_j \|^2 / 2\sigma_j^2)] \quad (j = 1, 2, \cdots, M) \tag{1}$$

Where $\boldsymbol{X} = [x_1, x_2, \cdots, x_n]^{\mathrm{T}}$ is n-dimensional input vector, $\boldsymbol{C}_j$ is the j-th basis function center which has the same dimension with the input vector, σ_j is the j-th perception variable which determines the basis function width, M is the perception unit number, $\|\cdot\|$ is Euclidean distance which is defined as follows

$$\| \boldsymbol{X} - \boldsymbol{C}_j \| = [(\boldsymbol{X} - \boldsymbol{C}_j)^T (\boldsymbol{X} - \boldsymbol{C}_j)]^{1/2} \tag{2}$$

According to formula (1), when the input vector $\boldsymbol{X}$ is located in the j-th hidden player unit center $\boldsymbol{C}_j$, then $\| \boldsymbol{X} - \boldsymbol{C}_j \| = 0$ and $\varphi_j(\boldsymbol{X}) = 1$. If $\boldsymbol{X}$ is far from $\boldsymbol{C}_j$, $\varphi_j(\boldsymbol{X})$ will be decrescendo. The output of hidden player unit j reflects the distance grade from $\boldsymbol{X}$ to the corresponding RBF center $\boldsymbol{C}_j$ which can be looked as a clustering center. The transmission function can produce major output only when the input vector locates in the region nearby the clustering center. So the transmission function works as a signal detector. σ_j is applied to adjust the clustering center range of action. σ_j becomes small, $\varphi_j(\boldsymbol{X})$ descends rapidly with $\| \boldsymbol{X} - \boldsymbol{C}_j \|$ increasing, the RBF transmission function output curve becomes very narrow and is sensitive to the input change; contrarily σ_j becomes big, the RBF transmission function output curve becomes gentle and is insensitive to the input change.

Due to the mapping from hidden player to output player is linear, the RBFNN output is the linear weight sum of hidden player unit output, which is shown as

$$y_k = \sum_{j=1}^{M} w_{kj} \cdot \varphi_j(\boldsymbol{X}), \ k = 1, 2, \cdots l \tag{3}$$

Converting formula (3) into matrix equation, the equation can be obtained as follows:

$$\boldsymbol{Y} = \boldsymbol{W} \cdot \boldsymbol{\Phi} \tag{4}$$

Where $\boldsymbol{Y} = [y_1, y_2, \cdots, y_l]^{\mathrm{T}}$ is l-dimensional output vector, $\boldsymbol{W} = [\boldsymbol{W}_1, \boldsymbol{W}_2, \cdots, \boldsymbol{W}_l]^{\mathrm{T}}$ is matrix of weight from hidden player to output player, $\boldsymbol{W}_k = [w_{k1}, w_{k2}, \cdots, w_{kM}]$ is the k-th unit weight vector of output player, $\boldsymbol{\Phi} = [\varphi_1(\boldsymbol{X}), \varphi_2(\boldsymbol{X}), \cdots \varphi_M(\boldsymbol{X})]^{\mathrm{T}}$ is the hidden player output vector.

2.2 Learning method

Seeing the RBFNN learning process, there are two methods for training, one is the hybrid mode, and the other is the supervised mode.

1. Hybrid mode

Moody and Darken proposed a hybrid method for RBFNN learning. Firstly, the RBF center is determined by unsupervised method after the number of radial basis functions is specified.

Secondly, the output player weight is determined by supervised method. According to the hybrid method in unsupervised stage, there are two common methods as follows:

(1) Random selecting RBF center

As a simplest method, the RBF centers in hidden player are selected randomly from input data samples and the centers are changeless. Due to the hidden player unit output is known, the network connection weights can be solved by linear equations.

If the Guass function is employed for RBF, it can be represented as follows:

$$\varphi(\|\boldsymbol{X}-\boldsymbol{C}_j\|)=\exp(-\frac{M}{d_m^2}\|\boldsymbol{X}-\boldsymbol{C}_j\|^2) \quad j=1,2,\cdots M \tag{5}$$

Where M is the number of centers (i.e., hidden player units), d_m is the max distance among the selected center. In this case, the mean square deviation (i.e., RBF width) can be specified as follows

$$\sigma=d_m/\sqrt{2M} \tag{6}$$

(2) Self-organization selecting RBF center

According to the multivariable interpolation RBF methods, the center $\boldsymbol{C}_j$ is usually located in the input vector point, so the hidden player units are consistent with the input data. Considering the input data maybe have clustering performance especially to the pattern recognition, there will be so many closed RBF centers that generates redundant points, the learning time become long, and the over fitting appears which leads to generalization ability debased. In order to overcome these problems, the input data are usually disposed by clustering analysis technology for selecting representation points as RBF centers, so the number of hidden player units is reduced and the structure complexity is debased. In this method, the RBF centers can move and be located by self-organization learning. The K-mean clustering algorithm which belongs to unsupervised method is usually employed for selecting RBF centers [20], the calculation steps are as follows:

(a) The clustering center $\boldsymbol{C}_j(j=1,2,\cdots,M)$ is initialized by selecting M samples from input samples $\boldsymbol{X}_i(i=1,2,\cdots,N)$.

(b) The input samples are classified according to the nearest neighbor rule. In this way, for that $\boldsymbol{X}_i$ is distributed to input sample clustering set $\boldsymbol{\theta}_j(j=1,2,\cdots,M)$ whose clustering center is $\boldsymbol{C}_j$, i.e., $\boldsymbol{X}_i\in\boldsymbol{\theta}_j$, and the condition need to be met

$$d_j=\min\|\boldsymbol{X}_i-\boldsymbol{C}_j\| \tag{7}$$

Where d_j is the min Euclidean distance.

Calculating the mean of samples in $\boldsymbol{\theta}_j$, i.e., the clustering center:

$$\boldsymbol{C}_j = \frac{1}{M_j} \sum_{\boldsymbol{X}_i \in \boldsymbol{\theta}_j} \boldsymbol{X}_i \tag{8}$$

Where M_j is the number of input samples in $\boldsymbol{\theta}_j$.

After obtained the centre $\boldsymbol{C}_j$ and RBF width σ_j, the RBFNN can be trained to adjust the weight matrix W for minimizing the solution object function. Due to the space mapping from hidden player to output player is linear, i.e., the network output is the weighted sum of hidden player unit output. The relationship between hidden player and output player can be represented the matrix as follows:

$$\boldsymbol{Y} = \boldsymbol{W} \cdot \boldsymbol{\Phi} = \boldsymbol{U} \tag{9}$$

Where $\boldsymbol{U}$ is the object vector. The weight matrix $\boldsymbol{W}$ can be calculated by linear optimization methods, e.g., the least square method [21]. Solving the pseudo-matrix for $\boldsymbol{\Phi}$ in the formula (9), the weight matrix can be obtained:

$$\boldsymbol{W} = \boldsymbol{U}\boldsymbol{\Phi}^{\mathrm{T}}(\boldsymbol{\Phi}\boldsymbol{\Phi}^{\mathrm{T}})^{-1} \tag{10}$$

2. Supervised mode

The RBF centers, width and output player weight are determined by supervised learning mode which is the general mode for RBFNN learning. The learning algorithm can be solved by gradient descent algorithm. The weight matrix $\boldsymbol{W}$ can be obtained by iterative algorithm follows gradient descent regulation. The iterative formula is calculated as follows:

$$\boldsymbol{W}(k+1) = \boldsymbol{W}(k) + \eta(\boldsymbol{U} - \boldsymbol{Y})\boldsymbol{\Phi}^{\mathrm{T}} \tag{11}$$

Where η is the learning factor. Due to the output is linear unit, the gradient descent algorithm can converge the global solution.

In the learning process, if the central nodes are so excess that the training time will increase and the network will be over fitting which debases the RBFNN generalization ability; if the central nodes are so insufficient that the training algorithm will not converge, so the nodes need to increase. For the supervised mode, the number of radial basis functions need to be specified before training, the training time is long and the training algorithm maybe not converges, and the initial condition maybe lead to the training algorithm converging in local minimum. In order to dispose the shortages mentioned above, some improved methods are proposed by researchers, e.g., the hybrid method based on gradient descent and least square algorithm, orthogonal least square algorithm [22]. Yet, there is local minimum problem for gradient descent method; the orthogonal least square is unfit for recursive calculation and the determination for RBF centers need further study.

3. Data acquisition system

According to the cooling dehumidifier work analysis, the inherent parameters such as suction temperature, suction pressure, discharge temperature, discharge pressure, evaporation temperature, evaporation pressure, condensation temperature, and condensation pressure mostly affect the dehumidifier work performance. In the normal condition, the evaporation temperature and evaporation pressure are corresponding, and this also to condensation temperature and condensation pressure; the evaporation pressure and suction pressure are approximate, and this also to condensation pressure and discharge pressure. Furthermore, extrinsic parameters also influence the dehumidifier work performance, and they affect the system by causing the inherent parameters changing. In this studied experimental system, the extrinsic parameters include air intake temperature, air intake humidity, air volume, compressor power, cooling water intake temperature and flow. According to these parameters, the dehumidifier data acquisition system is built by employing measurement sensors, transducers, peripheral component interconnect data acquisition card and upper computer. Based on the built system, the dehumidifier work status simulation, data acquisition, fault detection and diagnosis can be implemented.

The data acquisition system for a tempering cooling dehumidifier is built generally shown as Fig.3. The illustration of measurement parameters is shown as Tab.1. For the cooling dehumidifier, the nominal dehumidification capacity is 21 kg/h, the refrigeration capacity is 32.9 kW, and the input power is 7.7 kW. The requirement environment for dehumidifier normal work is that the temperature is in ranges of 18-32 °C and the RH is in ranges of 45%-90%. These measurement sensors in the data acquisition system include temperature sensors with accuracy of ±0.1 °C, RH sensors with accuracy of ±2%, pressure sensors with accuracy of ±0.02 bar, air velocity sensor with accuracy of ±0.2 m/s, flow sensor with accuracy of ±0.15 L/min, compressor power sensor with accuracy of ±0.02 kW. The measurement uncertainty is as follows: temperature, ±0.06 °C; RH, ±1.2%; pressure, ±0.01 bar; air velocity ±0.12 m/s; flow, ±0.1 L/min; compressor power, ±0.01 kW. All these sensors are calibrated before applications according to the requirement environment for dehumidifier work.

~~The time-step is set as 1s.~~

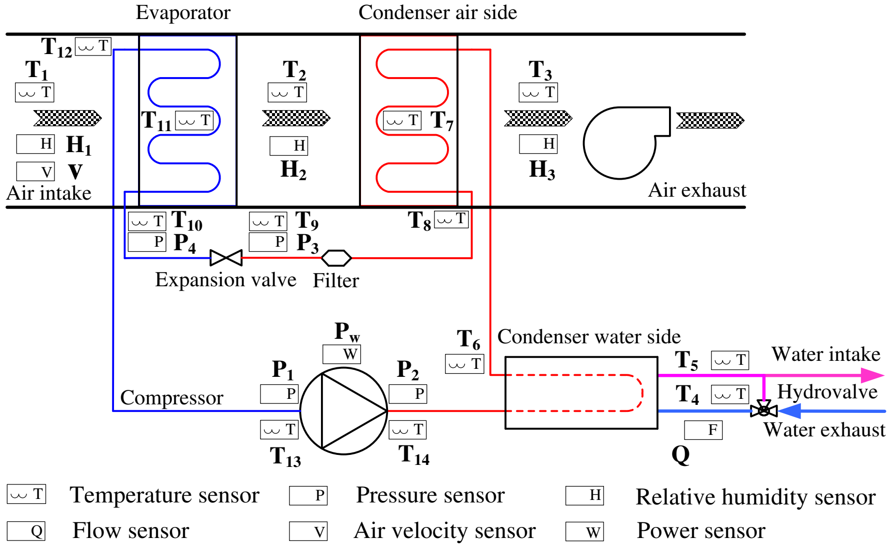

Fig.3 - The dehumidifier experimenta and measurement system.

Tab.1 - Illustration of measurement parameters.

Symbol	Measurement parameter	Symbol	Measurement parameter
T_1	Air intake temperature	T_{13}	Compressor suction temperature
T_2	Evaporator air exhaust temperature	T_{14}	Compressor discharge temperature
T_3	Condenser air exhaust temperature	H_1	Air intake relative humidity (RH)
T_4	Condenser water intake temperature	H_2	Evaporator air exhaust RH
T_5	Condenser water exhaust temperature	H_3	Condenser air exhaust RH
T_6	Condenser inlet temperature	P_1	Compressor suction pressure
T_7	Condensation temperature	P_2	Compressor discharge pressure
T_8	Condenser outlet temperature	P_3	Expansion valve inlet pressure
T_9	Expansion valve inlet temperature	P_4	Expansion valve outlet pressure
T_{10}	Expansion valve outlet temperature	V	Air velocity
T_{11}	Evaporation temperature	Q	Water flow
T_{12}	Evaporator outlet temperature	P_w	Compressor power

After the data acquisition system has been built, the dehumidifier work statuses in that refrigeration system faults commonly occur can be simulated by controlling the work condition and introducing artificial faults. These statuses include normal work, 9 kinds of single faults and 6 kinds of compound faults. The single faults include evaporator fouled, air cooling condenser fouled, air intake volume decrease, air intake filter fouled, air intake temperature lower, water intake volume overfull, refrigerant insufficient, expansion valve open oversize and undersize, and the compound faults include air cooling condenser fouled combined air intake volume decrease, evaporator fouled combined air intake volume decrease, air intake volume decrease combined water intake volume overfull, evaporator fouled combined water intake volume overfull, evaporator fouled combined air cooling condenser fouled and air cooling condenser fouled combined water intake volume overfull.

The dehumidifier work statuses simulation can be operated by introducing artificial faults. In the dehumidifier work statuses simulation process, it need to determine whether the dehumidifier works in steady by the measurement parameters change and steady detector [8] at first. If the simulated status works in steady state, then the measurement data can be acquired and recorded for fault analysis and diagnosis.

4. Optimization for RBFNN

For the problem of building model, the calculation time and storage space will be increased by geometric progression with the sample number and dimension increasing. So effectively extracting feature becomes an important problem for building system model. By feature extraction, the complexity of learning problem can be debased, the generalization ability can be improved, and the learning model can be simplified. Principle component analysis (PCA) is a multivariate statistical analysis technology for data compression and information extraction [23, 24], it is suitable for analyzing multidimensional process variable and the data set composed of other elements which affect the process operation. Before building system model, employing PCA method can furthest preserve the useful information, eliminate the relationship from variables, and filter redundant information. Although PCA is an effective feature extraction method, it is virtually a linear mapping. The KPCA method combines PCA and kernel method not only fits for disposing the nonlinear problem but also supplies more information [25, 26]. For the HVAC&R system, the nonlinear characteristic is obvious, there are strong coupling among characteristic variables especially when the compound faults occur. KPCA can better relieve the nonlinear relevancy among variables so that it can better solve the compound fault problem.

Genetic algorithm (GA) is a self-adapting global optimization and probability searching algorithm, which imitates the mechanism of biology evolution such as natural selection and genetic variation. Due to the main characteristic of GA are population searching strategy, information interchange and searching independent on gradient information, GA is very suitable for solving nonlinear problem [27-29], thus it has been applied to many fields such as machine learning, function optimization, pattern recognition and automatic control. Based on the merits of GA, it can be employed for ANN aided design and optimization which will improve the ANN performance [30].

4.1 Data dimensionality reduction by KPCA

The main idea of KPCA is that calculate the principle component in the feature space which is mapped from input space by nonlinear mapping. KPCA employs a simple kernel function for finding a countable and controllable solution, this means that construct a nonlinear mapping from input space to feature space. So KPCA is a nonlinear PCA accomplished in input space. If the purpose of PCA application is diagonalizing the covariance matrix, weakening the nonlinear relationship in the given data set $\boldsymbol{x}_k \in \boldsymbol{R}^m (k = 1, 2, \cdots, N)$, the covariance can be represented in linear feature but not nonlinear input space, i.e.,

$$\boldsymbol{C}^F = \frac{1}{N}\sum_{i=1}^{N}\varphi(\boldsymbol{x}_i)\varphi(\boldsymbol{x}_i)^{\mathrm{T}} \tag{12}$$

Here, supposing $\sum_{i=1}^{N}\varphi(\boldsymbol{x}_i) = 0$, and $\varphi(\cdot)$ is a nonlinear mapping function which maps the variable from input space to F feature space. In order to diagonalize the covariance matrix, it need to resolve the eigenvalue in feature space:

$$\lambda \boldsymbol{v} = \boldsymbol{C}^F \boldsymbol{v} \tag{13}$$

The eigenvalue $\lambda > 0$, and $\boldsymbol{v} \in \boldsymbol{F} \neq \{0\}$. $\boldsymbol{C}^F \boldsymbol{v}$ can be represented as follows:

$$\boldsymbol{C}^F \boldsymbol{v} = \left(\frac{1}{N}\sum_{i=1}^{N}\varphi(\boldsymbol{x}_i)\varphi(\boldsymbol{x}_i)^{\mathrm{T}}\right)\boldsymbol{v} = \frac{1}{N}\sum_{i=1}^{N}\langle\varphi(\boldsymbol{x}_i), \boldsymbol{v}\rangle\varphi(\boldsymbol{x}_i) \tag{14}$$

Where $\langle \boldsymbol{x}, \boldsymbol{y} \rangle$ denotes inner product of $\boldsymbol{x}$ and $\boldsymbol{y}$. This indicates the solution $\boldsymbol{v}$ corresponding to λ must locate in the subspace spanned $\varphi(\boldsymbol{x}_1), \varphi(\boldsymbol{x}_2) \cdots, \varphi(\boldsymbol{x}_N)$. So $\lambda \boldsymbol{v} = \boldsymbol{C}^F \boldsymbol{v}$ is equivalent to

$$\lambda\langle\varphi(\boldsymbol{x}_k), \boldsymbol{v}\rangle = \langle\varphi(\boldsymbol{x}_k), \boldsymbol{C}^F \boldsymbol{v}\rangle \quad k = 1, 2, \cdots N \tag{15}$$

and there will be factor $a_j (j = 1, 2, \cdots N)$ to make

$$\boldsymbol{v} = \sum_{j=1}^{N} a_j \varphi(\boldsymbol{x}_j) \tag{16}$$

Synthesizing formula (12), (15) and (16), the following formula can be obtained:

$$\lambda\sum_{j=1}^{N} a_j \langle\varphi(\boldsymbol{x}_k), \varphi(\boldsymbol{x}_j)\rangle = \frac{1}{N}\sum_{j=1}^{N} a_j \left\langle\varphi(\boldsymbol{x}_k), \sum_{i=1}^{N}\varphi(\boldsymbol{x}_i)\right\rangle\langle\varphi(\boldsymbol{x}_i), \varphi(\boldsymbol{x}_j)\rangle \tag{17}$$

The eigenvalue problem only introduces the inner product of mapping vector in feature space demonstrated in formula (17).

Defining a $N \times N$ order kernel matrix $\boldsymbol{K}$, where matrix element $K_{ij} = \varphi(\boldsymbol{x}_i)^{\mathrm{T}} \varphi(\boldsymbol{x}_j)$, $1 \le i \le N$, $1 \le j \le N$. Noticing $\boldsymbol{K}$ is a symmetry matrix, formula (17) can be simplified as follows:

$$N\lambda\boldsymbol{\alpha} = \boldsymbol{K}\boldsymbol{\alpha} \tag{18}$$

The feature vector $\boldsymbol{v}$ of $\boldsymbol{C}^F$ can be solved by the feature vector $\boldsymbol{\alpha}$ of $\boldsymbol{K}$, i.e., the principle component direction of mapping space.

In this way, the principle component $\boldsymbol{t}$ of test vector $\boldsymbol{x}$ in the input space is extracted by $\varphi(\cdot)$ mapping to feature vector $\boldsymbol{v}_k$ in F space:

$$\boldsymbol{t}_k = \langle \boldsymbol{v}_k, \varphi(\boldsymbol{x}) \rangle = \sum_{j=1}^{N} a_j^k \langle \varphi(\boldsymbol{x}_j), \varphi(\boldsymbol{x}) \rangle \tag{19}$$

Where $k = 1,2,\Lambda\ p$, and p is the principle component number which can be calculated according to the following formula:

$$\sum_{k=1}^{p} \lambda_k / \sum_{k=1}^{m} \lambda_k \ge C \tag{20}$$

Where m is the eigenvalue number, and C is a constant spanned 0.85-0.95, here assigned 0.90.

Introducing the inner product kernel function shown as the following formula to feature space can avoid directly calculating nonlinear mapping

$$K(\boldsymbol{x}_i, \boldsymbol{x}_j) = \langle \varphi(\boldsymbol{x}_i), \varphi(\boldsymbol{x}_j) \rangle = \varphi(\boldsymbol{x}_i)^{\mathrm{T}} \varphi(\boldsymbol{x}_j) \tag{21}$$

Selection of kernel function entirely determines the mapping φ and feature F, the common kernel functions [31] includes:

(1) Guass radial basis function

$$K(\boldsymbol{x}, \boldsymbol{x}_i) = \exp\left(-\frac{\|\boldsymbol{x} - \boldsymbol{x}_i\|^2}{2\sigma^2} \right) \tag{22}$$

(2) q order polynomial function

$$K(\boldsymbol{x}, \boldsymbol{x}_i) = (\boldsymbol{x}^{\mathrm{T}} \boldsymbol{x}_i + 1)^q \tag{23}$$

(3) two players perceptron function

$$K(\boldsymbol{x}, \boldsymbol{x}_i) = \tanh(\beta_0 \boldsymbol{x}^{\mathrm{T}} \boldsymbol{x}_i + \beta_1) \tag{24}$$

In this paper, the Gauss radial basis function is employed for KPCA kernel function.

4.2 Structure and parameter optimized by AGA

In GA the possible solution of problem field is considered as one individual or chromosome, and every individual is encoded in the character string form. It repeatedly operates the population based on genetics by imitating the process of genetic selection and nature elimination according to the biology evolution mechanism. Every individual is evaluated depended on the preset object fitness function, and the optimal population is obtained according to the principle that the excellent one exists and the inferior one eliminates. At the same time, the optimal individual in the optimal population is obtained by the global parallel search, which is the optimal solution being satisfied to the requirement. The standard GA flow is shown as Fig.4.

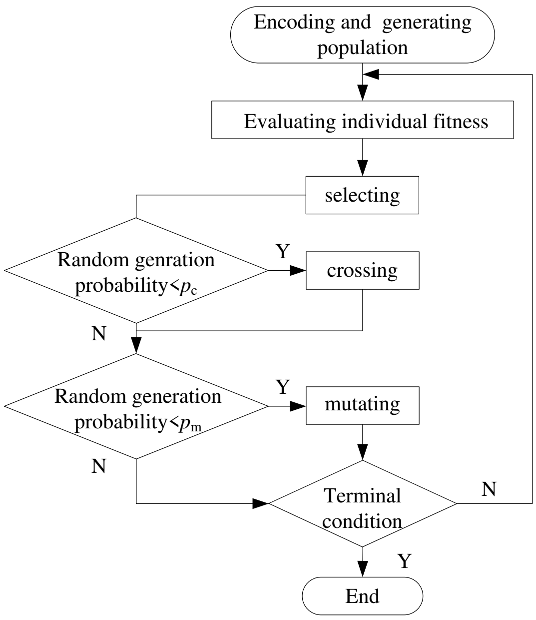

Fig.4 - Flow of standard GA.

Parameter encoding, fitness function setting, genetic operating, initial population setting and control parameters setting are the basic components of GA, and the selection, cross and mutation are the basic operations of GA.

In GA control parameters, how to select the cross probability p_c and the mutation probability p_m is very important, because they influence the algorithm performance. Unsuitable selecting for p_c and p_m will not lead to search the optimal solution. Due to control parameters in standard genetic algorithm are fixed, it will not make full use of the three genetic operators, which results in the algorithm being in premature convergence state or getting in local minimum state. Especially the repeating selection for p_c and p_m by experiment is a fussy work, and it is difficult to find the optimal values for them. Based on this problem, Srinvivas and Patnaik [32] proposed an AGA which is improved by other researchers. According to the idea of AGA, p_c and p_m are automatically changing along with the fitness. They are calculated as follows:

$$p_c = \begin{cases} p_{c1} - \dfrac{(p_{c1} - p_{c2})(f' - f_{avg})}{f_{max} - f_{avg}}, & f' \geq f_{avg} \\ p_{c1}, & f' < f_{avg} \end{cases} \tag{25}$$

$$p_m = \begin{cases} p_{m1} - \dfrac{(p_{m1} - p_{m2})(f_{max} - f)}{f_{max} - f_{avg}}, & f \geq f_{avg} \\ p_{m1}, & f < f_{avg} \end{cases} \tag{26}$$

Where f_{max} is the max value of all the population's fitness, f_{avg} is the average fitness value of every generation population, f' is the bigger fitness value of the two crossover individuals, f is the fitness value of the mutation individual; p_{c1} value is 0.9, p_{c2} value is 0.6, p_{m1} value is, and p_{m2} value is 0.006.

In view of the limitations in the RBFNN learning methods based on gradient descent algorithm, this paper employs a hybrid learning method based on K-means clustering algorithm for training the RBFNN. But in this conventional K-means clustering algorithm, the initial clustering number M (i.e., the RBF number in hidden player) and the RBF width σ need to be artificially specified according to the experience in advance, which implies that there would be some human subjectivity. When the learning effect is not ideal, these two parameters need to be adjusted repeatedly which leads to the fussy operation and bad practicability. For this problem, this study proposed a hybrid learning algorithm based on AGA which employs AGA for automatically selecting the parameters of M and σ, the RBF centers are determined by K-means clustering and the output player weights are determined by least square algorithm. This proposed method not only overcomes the local minimum in the conventional K-means clustering algorithm, but also automatically selects the RBF number and width which overcomes the blindness and subjectivity in the artificial selection method for these parameters in theory. Moreover, this method achieves a perfect balance between the RBFNN structure and output precision due to employing K-means clustering algorithm optimized by AGA, and the overfitting problem is overcame in some degrees, thus the ANN model generalization ability is improved.

In this paper, the genetic resolving procedure is as follows:

(1) Encoding.

The parameters of M and σ are encoding in real form, the span of former is $[1, N/2]$ and the span of latter is $[0.01,5]$, where N is the total number of samples.

(2) Fitness function designing.

The fitness function is designed as

$$fit_{\mathrm{RBF}} = \frac{1}{\sum_{i=1}^{N}\sum_{j=1}^{l}(d_{ij} - y_{ij})^2 + 1} \tag{27}$$

Where d_{ij} is the j-th expectation output corresponding to the i-th sample, y_{ij} is the real output corresponding to d_{ij}; N is the number of learning samples and l is the number of output player units.

(3) Genetic operating.

The selection operation employs roulette operator, and the optimal preserving strategy is employed. The crossover operation employs arithmetic crossover operator, and the mutation operation employs nonuniform mutation operator. The crossover probability p_{c} and mutation probability p_{m} are adaptively calculated according to the AGA.

(4) Other enactment.

The initial population generated at random, and the scale is 40 based on considering the resolving speed; the algorithm is terminated until the generations achieve to 200.

5. Application for fault diagnosis

Firstly, the normal and fault work statuses of the dehumidifier are simulated, and the data under each steady state work status are collected by the data acquisition system as the fault sample database. Secondly, fault samples are selected to train and optimize the RBFNN model. Thirdly, the RBFNN model is validated until it meets the requirement of application precision. Finally, the model is applied to fault diagnosis, the disposed real-time data samples acquired from the dehumidifier are inputted into the RBFNN model for calculation, and the faults are diagnosed by the model output results. It should be pointed out that when the dehumidifier has new faults, the diagnosis result is inconsistent with the actual status, the work environment or the dehumidifier configuration has changed, the sample database needs to be updated and then the RBFNN model needs to be retrained and revalidated to ensure the effectiveness and reliability of fault diagnosis. The flow of RBFNN trained and employed for fault diagnosis is shown as Fig.5.

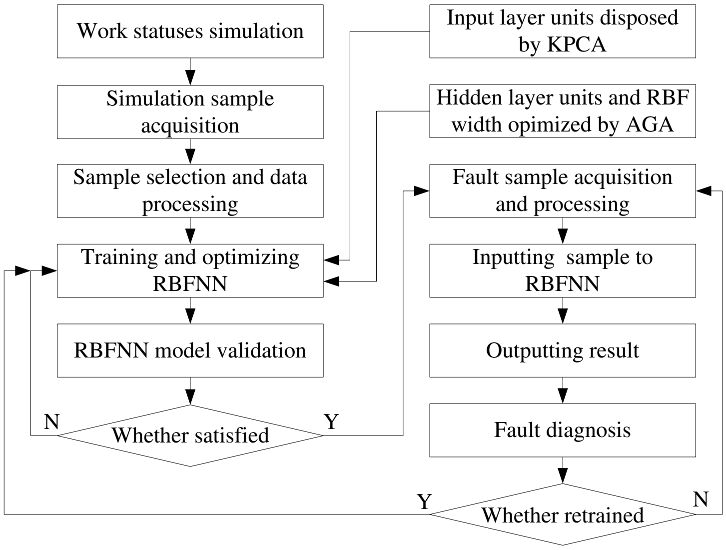

Fig.5 - The flow of RBFNN learning and application.

Before the RBFNN is trained and applied, the input data sample needs to be normalized to the [-1, 1] span in order to decrease the computational complexity and model error to prevent the model oscillation. After the model finishes calculation, the output result needs to be renormalized.

In order to eliminate the influence from outside interference to data fluctuation, the input data is smoothed by the moving average method for improving modeling precision and fault diagnosis accuracy before the data normalized.

The normalization is calculated as:

$$x_k = \frac{b-a}{\max x_{k0} - \min x_{k0}}(x_{k0} - \min x_{k0}) \tag{28}$$

Where x_{k0} is original data, $\max x_{k0}$ is the max value of input data, and $\min x_{k0}$ is the minimum value of input data, b is the max value of normalization span, a is the min value of normalization span, and $b=1$, $a=-1$.

The moving average is calculated as:

$$\overline{x}_k = \sum_{i=-q}^{p} \omega_i x_{k+i} \tag{29}$$

Where x_{k+i} is the original measurement data, ω_i is the weight factor, and $\sum_{i=-q}^{p} \omega_i = 1$, $k = q+1, q+2, \cdots, N-p$, p and q are respectively arbitrary positive integer which is less than the smooth span m, and $p+q+1=m$, N is the number of measurement data.

In order to correctly identify the dehumidifier work statuses mentioned above and improve the RBFNN generalization ability, the training sample is selected according to the rule: 100 groups of samples are selected corresponding to every work status; every group of sample selects 18 work parameters, which are compressor suction temperature, suction pressure, discharge temperature, discharge pressure, dehumidifier air intake velocity, air intake temperature, air exhaust temperature, dehumidifier air intake RH , air exhaust RH, condenser water intake flow, water intake temperature, water exhaust temperature, condensing temperature, expansion valve inlet temperature, evaporator inlet temperature, evaporating temperature, evaporator air exhaust temperature and compressor power.

Obviously, if all these parameters are selected as the sample dimension, the RBFNN structure would be large and the training would be complex. So here employs KPCA for extracting input data sample feature in order to reduce the data sample dimension. According to formula (20), when the kernel function width σ is assigned 0.3441, the calculation result of principle components number is 7, i.e., the number of input player units corresponding to 7 principle components extracted by KPCA is 7. The output player units are 16 bits which respectively corresponds to the dehumidifier work statuses, i.e., if the input sample is corresponding to the i-th (1≤i≤16) work status, then the i-th bit value is 1 and the other bits value are 0, here the whole output bits can be represented as $[\overset{1}{0}\,\overset{2}{0} \cdots \overset{i}{1} \cdots \overset{15}{0}\,\overset{16}{0}]$. The relationship of RBFNN outputs corresponding to work statuses is illustrated as Tab. 2.

Tab. 2 - The relationship of RBFNN outputs corresponding to work statuses.

Work status No.	Fault mode	RBFNN output
1	Normal	1 0 0 0 0 0 0 0 0 0 0 0 0 0 0 0
2	Evaporator fouled	0 1 0 0 0 0 0 0 0 0 0 0 0 0 0 0
3	Air cooling condenser fouled	0 0 1 0 0 0 0 0 0 0 0 0 0 0 0 0
4	Air intake volume decrease	0 0 0 1 0 0 0 0 0 0 0 0 0 0 0 0
5	Air intake filter fouled	0 0 0 0 1 0 0 0 0 0 0 0 0 0 0 0
6	Air intake temperature lower	0 0 0 0 0 1 0 0 0 0 0 0 0 0 0 0
7	Water intake volume overfull	0 0 0 0 0 0 1 0 0 0 0 0 0 0 0 0
8	Refrigerant insufficient	0 0 0 0 0 0 0 1 0 0 0 0 0 0 0 0
9	Expansion valve open oversize	0 0 0 0 0 0 0 0 1 0 0 0 0 0 0 0
10	Expansion valve open undersize	0 0 0 0 0 0 0 0 0 1 0 0 0 0 0 0
11	Air cooling condenser fouled + air intake volume decrease	0 0 0 0 0 0 0 0 0 0 1 0 0 0 0 0
12	Evaporator fouled + air intake volume decrease	0 0 0 0 0 0 0 0 0 0 0 1 0 0 0 0
13	Air intake volume decrease + water intake volume overfull	0 0 0 0 0 0 0 0 0 0 0 0 1 0 0 0
14	Evaporator fouled + water intake volume overfull	0 0 0 0 0 0 0 0 0 0 0 0 0 1 0 0
15	Evaporator fouled + air cooling condenser fouled	0 0 0 0 0 0 0 0 0 0 0 0 0 0 1 0
16	Air cooling condenser fouled + water intake volume overfull	0 0 0 0 0 0 0 0 0 0 0 0 0 0 0 1

Employing the hybrid learning method expounded in section 4 (i.e., Optimization for RBFNN) for RBFNN training and optimizing, it can obtain the RBFNN structure and parameters. The change of AGA fitness function value in solving process is shown as Fig.6.

The AGA converges in the 173 generation, and the offline training time of the algorithm is 190.3342 seconds. The best individual fitness value is 0.9953, and then the best solution can be obtained, where the number of radial basis functions (i.e., the hidden player neurons) M=757, and the RBF width σ=0.3441. The mean square error (MSE) of the RBFNN obtained is 1.8359×10^{-7}。

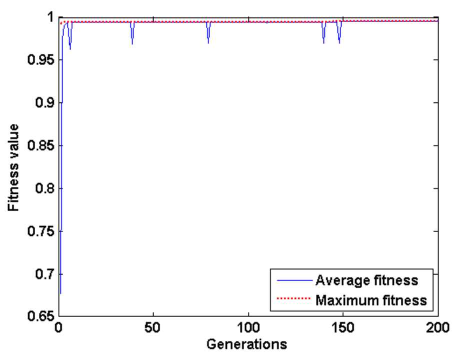

Fig.6 - Fitness function value change in solving process.

Corresponding to the 16 kinds of dehumidifier work statuses, 16 groups of test samples besides the training samples are selected to input the trained RBFNN for model validation and verify the model generalization ability, the 16 groups of output results are shown as Fig.7, and the online running time of the trained model is 3.8150×10^{-3} second. As demonstrated in Fig.7, the *i*-th ($1\leq i\leq16$) bit value is 1 (rounded to integer) and other bits value are 0 (rounded to integer) in each output result, which indicates that the output result corresponds to the *i*-th work status illustrated in Tab. 2 and the fault modes corresponding to the input samples are correctly identified.

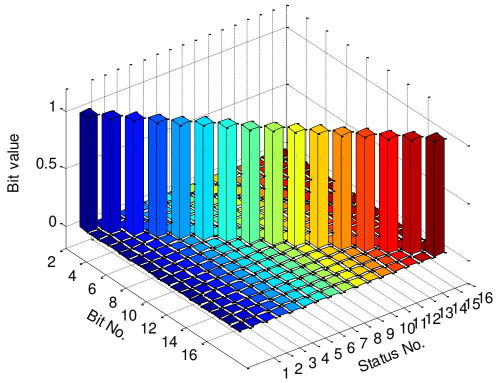

Fig.7 - Model validation result for fault diagnosis.

In order to verify the RBFNN application effect, corresponding to each work status, 16 groups of fault data samples acquired from the dehumidifier data acquisition system are selected for inputting the RBFNN to calculate, the 16 groups of output results are shown as Fig.8. As demonstrated in Fig.8, each output result is consistent with the factual work status (i.e., fault mode) corresponding to the data sample. This indicates the RBFNN model proposed in this paper has favorable fault recognition ability that can correctly recognize not only the single but also the compound fault, and it needs to be referred that the compound fault is more difficult for fault diagnosis due to the close coupling of equipment status parameters, e.g., If the air intake volume decrease fault occurs, then the evaporation pressure drops and the condensation pressure rises. If the compound fault of evaporator fouled + air cooling condenser fouled occurs, then the evaporation pressure maybe drops and the condensation pressure maybe rises. Due to the coupling relationship between evaporation and condensation pressure, both the evaporation and condensation pressure maybe drop or rise at the same time, even one of them may be changeless. Therefore, it is relatively difficult for accurately discriminating the single fault of air intake volume decrease and the compound fault of evaporator fouled + air cooling condenser fouled. Moreover, it is also difficult for recognizing the compound fault of evaporator fouled + air cooling condenser fouled. As can be seen, employing the common methods to diagnose these two single and compound faults is hard, even though these two faults are discriminated, it will need a lot of detailed and trustworthy expert knowledge which is not easily acquired in engineering.

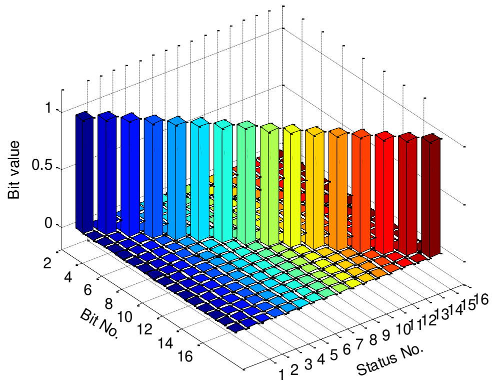

Fig.8 – Test of fault diagnosis for data samples.

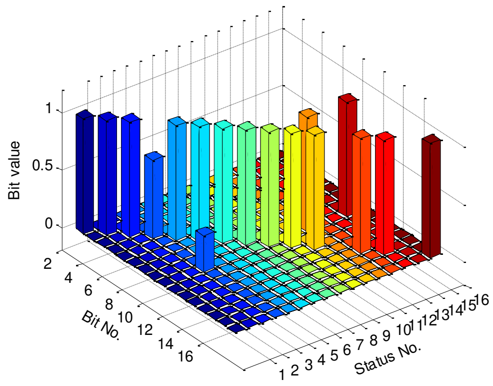

Fig.9 –Fault diagnosis test by model 1.

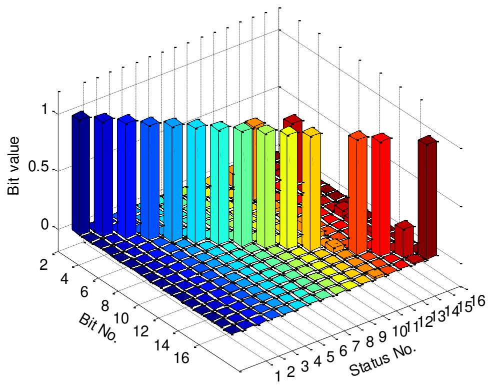

Fig.10 –Fault diagnosis test by model 2.

In order to further illustrate the advantages of this proposed method, here is a comparative analysis with the two conventional RBFNN models. The first model employs the direct creation method (defined as model 1), the number of neurons in the hidden layer is equal to the number of input samples, and the centers are the data sample points; the second model employs the step-by-step creation method (defined as model 2). The number of neurons in the hidden layer gradually increases from zero according to the error, and the increased neuron center are the sample point with the maximum error, the model stops training until it meets the set accuracy conditions. The width of RBF in the two models is selected according to experience, and the parameter value is 0.25. It should be pointed out that in order to obtain the ideal RBFNN model, the width of RBF needs to be adjusted repeatedly according to the experiment, and the operation is cumbersome, which brings inconvenience to the application. The same data samples are used to train and validate these two models, and the validated results are respectively shown in Fig.9 and Fig.10. Compared with Fig.8, the classification precision of Fig.9 and Fig.10 significantly decreases, and even there is the phenomenon of misclassification, where these two models respectively classify fault mode12 and fault mode15 into fault mode 9 and fault mode 4. From the comparison, it can be seen that the RBFNN model proposed in this paper has prominent advantages in the accuracy of compound fault diagnosis than the conventional RBFNN models.

6. Conclusions

In this paper, the diagnosis for cooling dehumidifier compound fault is studied and explored. Due to the obvious nonlinear characteristics of the refrigeration system and the strong coupling between various components in the work, it is difficult to establish a model for compound fault diagnosis. In view of the strong nonlinear processing ability of ANN, this paper proposed a compound fault diagnosis method for cooling dehumidifier based on RBFNN improved by KPCA and AGA. On the one hand, AGA and K-means clustering algorithm are used to automatically optimize the RBF width, the number of neurons in the hidden layer and the neuron center. On the premise of ensuring that the RBFNN model has sufficient output accuracy, it has a smaller structure and faster online calculation speed, which solves the problems that the selection of RBF width depends on expert knowledge, large network structure or slow training speed in the traditional RBFNN method; On the other hand, KPCA is employed to reduce the dimension of the model input data, eliminate the correlation between variables, and further optimize the network structure while effectively extracting nonlinear features. In order to illustrate the advantages of this research method, it is compared with two traditional RBFNN methods for performance analysis by employing the same modeling, testing and diagnosis samples. The comparison results show that this proposed method can not only be effectively applied to the compound fault diagnosis for the cooling dehumidifier, but also has obvious application advantages compared with other RBFNN methods.

7. Discussions

Objectively speaking, the inherent problems of cooling dehumidifier lead to us working hard for the compound fault diagnosis, e.g., the influence of outside interference, the close coupling of inner parameters, the fault artificial simulation difficulty, and so on. All these factors will affect the reliability of fault diagnosis. This study introduces three steps for eliminating these influences for fault diagnosis to sum up, firstly the model built data are coming from the dehumidifier multiple work statuses by artificial simulation in experiment; secondly the model input data are coming from the steady state and smoothed by the moving average method; lastly the strong fault tolerant and generalization ability of RBFNN are applied to restrain the outside interference to the model. These measures mentioned above ensure the RBFNN model application reliability for dehumidifier fault diagnosis, but the problem of inner mechanism of compound fault, work status simulation, fault profound diagnosis and so on need to deeply research.

The proposed RBFNN model employs AGA and K-means clustering algorithm to optimize the RBF width, the number of neurons in the hidden layer and the neuron center, and further employs KPCA to reduce the dimension of the input data, so that the model has a small structure on the premise of sufficient accuracy, thus ensuring the computing speed of the online application. By the group calculation of AGA, the best individual obtained is equivalent to performing multiple operations on the K-means clustering algorithm, and the optimal clustering result is selected as the neuron center in the network hidden layer. At the same time, it also restrains the problem that the K-means clustering algorithm is sensitive to the initialization value and easy to fall into the local minimum.

Although this paper has made a successful exploration in dehumidifier compound fault, there are still some work to be carried out in the further. For the compound fault diagnosis, this paper mainly researches two single faults combination situation due to the objective condition such as work status simulation limited. Theoretically speaking, though there is the relatively lower probability that three or more single faults occur simultaneously, it is still need to research, and the faults of different magnitude also need to research in the further.

This study mainly focuses on fault diagnosis in steady state, but the equipment work state maybe transform due to control, outside interference and other influence factors, although the equipment work parameters fluctuation and strong coupling bring more difficulties to fault diagnosis in unsteady state, it still needs further research.

In recent years, the application of artificial intelligence technology has promoted the research and development of deep learning ANN [33-38]. Among them, convolutional neural network (CNN) and long short-term memory (LSTM) neural network are the most typical structures. CNN can effectively extract the hidden features of high-dimensional data, and its unique network structure can reduce the number of parameters and data complexity while retaining data features, the deep fault characteristics are learned through multi-level nonlinear mapping relationship. However, CNN was originally used to process two-dimensional image data, and its specific application in fault diagnosis for one-dimensional time series needs further research. Recurrent neural network (RNN) can learn historical information and is very suitable for dealing with time series problems. As an improved RNN, LSTM network makes up for the difficult training problems such as gradient disappearance and explosion of ordinary RNN, and its practicability is further improved. In the further work, these two structural ANN can be studied for applications in fault diagnosis and prognosis according to their characteristics. Like other network models, the optimization of structure and parameters of these two ANN models also need to be studied.

8. Acknowledgments

The authors would be like to thank all scholars and engineers who previously provided theory and technique support.

9. References

[1] Lee S.H., Yik F.W.H.. A study on the energy penalty of various air-side system faults in buildings, Energy and Buildings. 2010, 42, 2-10.

[2] Yoshida H., Kumar S.. ARX and AFMM model-based on-line real-time data base diagnosis of sudden fault in AHU of VAV system, Energy Conversion & Management. 1999, 40, 1191-1206.

[3] Katipamula S., Brambley M.R.. Methods for Fault Detection, Diagnostics, and Prognostics for Building Systems-A Review, Part I, HVAC&R Research. 2005, 11, 3-25.

[4] Katipamula S., Brambley M.R.. Methods for Fault Detection, Diagnostics, and Prognostics for Building Systems-A Review, Part II, HVAC&R Research. 2005, 11, 169-187.

[5] Peitsman H.C., Bakker V.. Application of black-box models to HVAC systems for fault

detection, ASHRAE Transactions. 1996, 102, 628-640.

[6] Haves P., Salsbury T.I., Wright J.A.. Condition monitoring in HVAC subsystems using first principles, ASHRAE Transactions. 1996, 102, 519-527.

[7] House J.M., Lee W.Y., Shin D.R.. Classification Techniques for Fault Detection and Diagnosis of an Air-Handling Unit, ASHARET Transactions. 1999, 105, 1087-1097.

[8] Lee W.Y., House J.M., Kyong N.. Subsystem level fault diagnosis of a building's air-handling unit using general regression neural networks, Applied Energy. 2004, 77, 153-170.

[9] Du Z.M., Jin X.Q., Yang Y.Y.. Fault diagnosis for temperature, flow rate and pressure sensors in VAV systems using wavelet neural network, Applied Energy. 2009, 86, 1624-1631.

[10] Du Z.M., Fan B., Jin X.Q., Chi J.L.. Fault detection and diagnosis for buildings and HVAC systems using combined neural networks and subtractive clustering analysis, Building and Environment. 2014, 73, 1-11.

[11] Fan B., Du Z.M., Jin X.Q., Yang X.B., Guo Y.B.. A hybrid FDD strategy for local system of AHU based on artificial neural network and wavelet analysis, Building and Environment. 2010, 45, 2698-2708.

[12] Kamar H.M., Ahmad R., Kamsah N.B., Mustafa A.F.M.. Artificial neural networks for automotive air-conditioning systems performance prediction, Applied Thermal Engineering. 2013, 50, 63-70.

[13] Mohammad A.T., Mat S.B., Sulaiman M.Y., Sopian K., Al-abidi A.A.. Artificial neural network analysis of liquid desiccant dehumidifier performance in a solar hybrid air-conditioning system, Applied Thermal Engineering. 2013, 59, 389 -397.

[14] Jani D.B., Mishra M., Sahoo P.K.. Performance prediction of solid desiccant-Vapor compression hybrid air-conditioning system using artificial neural network, Energy. 2016, 103, 618-629.

[15] Gao Y.G., Liu S.B., Li F., Liu Z.G.. Fault detection and diagnosis method for cooling dehumidifier based on LS-SVM NARX model, International Journal of Refrigeration. 2016, 61, 69-81.

[16] Chen Y., Ji H.Q., Liu H.L., Sun L.Z.. A traffic identification based on PSO-RBF neural network in peer-to-peer network, International Journal of Computational Science and Engineering. 2016, 13, 158-164.

[17] Wei D.F.. Network traffic prediction based on RBF neural network optimized by improved gravitation search algorithm, Neural Computing & Applications. 2017, 28: 2303-2312.

[18] Moody J.E., Darken C.J.. Fast learning in networks of locally-tuned processing units, Neural Computation. 1989, 1, 281-294.

[19] Chiddarwar S.S., Babu N.R.. Comparison of RBF and MLP neural networks to solve inverse kinematic problem for 6R serial robot by a fusion approach, Engineering Applications of Artificial Intelligence. 2010, 23, 1083-1092.

[20] Pecháč P., Sága M.. Memetic algorithm with normalized RBF ANN for approximation of objective function and secondary RBF ANN for error mapping, Procedia Engineering. 2017, 177, 540-547.

[21] Gonzalez J., Rojas I., Pomares H.. A New Clustering Technique for Function Approximation, IEEE Transactions on Neural networks. 2002, 13, 132-142.

[22] Qian X.H., Huang H., Chen X.P., Huang T.G.. Generalized Hybrid Constructive

Learning Algorithm for Multioutput RBF Networks, IEEE Transactions on Cybernetics. 2017, 47, 3634-3648.

[23] Chen Y.M., Lan L.L.. A fault detection technique for air-source heat pump water chiller/heaters, Energy and Buildings. 2009, 41, 881-887.

[24] Han H., Cao Z.K., Gu B., Ren N.. PCA-SVM-Based Automated Fault Detection and Diagnosis (AFDD) for Vapor-Compression Refrigeration Systems, HVAC&R Research. 2010,16, 295-313.

[25] Schölkopf B., Smola A., Müller K.R.. Nonlinear component analysis as a kernel eigenvalue problem. Neural Computation. 1998, 10, 1299-1319.

[26] Cao L.J., Chua K.S., Chong W.K.. A Comparison of PCA, KPCA and ICA for Dimensionality Reduction in Support Vector machine, Neurocomputing. 2003, 55, 321-336.

[27] Palmes P.P., Hayasaka T., Usui S.. Mutation-based genetic neural networks, IEEE Transactions on neural Networks. 2005, 16, 587-600.

[28] Ashena R., Moghadasi J.. Bottom hole pressure estimation using evolved neural networks by real coded ant colony optimization and genetic algorithm, Journal of Petroleum Science and Engineering. 2011,77, 375-385.

[29] Irani R., Nasimi R.. Evolving neural network using real coded genetic algorithm for permeability estimation of the reservoir, Expert Systems with Applications. 2011, 38, 9862-9866.

[30] Balaga H., Gupta N., Vishwakarma D.N.. GA trained parallel hidden layered ANN based differential protection of three phase power transformer, Electrical Power and Energy Systems. 2015, 67, 286-297.

[31] Wu J.N., W J., Lui L.. Feature extraction via KPCA for classification of gait patterns, Human Movement Science. 2007, 26, 393-411.

[32] Srinivas M., Patnaik L.M.. Adaptive Probabilities of Crossover and Mutation in Genetic Algorithms, IEEE Transactions on Systems, Man and Cybernetics. 1994, 24, 656-667.

[33] Pouyanfar S., Sadiq S., Yan Y., Tian H., Iyengar S.S.. A survey on deep learning: algorithms, techniques, and applications. Acm Computing Surveys. 2018, 51, 1-36.

[34] Ye, Z., Yu, J.B.. Deep morphological convolutional network for feature learning of vibration signals and its applications to gearbox fault diagnosis. Mechanical Systems & Signal Processing. 2021, 161, 1-17.

[35] Chen S., Ge H., Li H., Sun Y., Qian X.. Hierarchical deep convolution neural networks based on transfer learning for transformer rectifier unit fault diagnosis. Measurement. 2021, 167, 1-21.

[36] Khorram A., Khalooei M., Rezghi M.. End-to-end CNN plus LSTM deep learning approach for bearing fault diagnosis. Applied Intelligence. 2021, 51, 736-751.

[37] Belagoune S., Bali N., Bakdi A., Baadji B., Atif K.. Deep learning through LSTM classification and regression for transmission line fault detection, diagnosis and location in large-scale multi-machine power systems. Measurement, 2021, 177, 1-14.

[38] Chen Y., Dong Z., Wang Y., Jie S., Han Z., Zhou D., Zhang K., Zhao Y., Bao Y.. Short-term wind speed predicting framework based on EEMD-GA-LSTM method under large scaled wind history. Energy conversion & management. 2021, 227, 1-16.